Copyright is owned by the Author of the thesis. Permission is given for a copy to be downloaded by an individual for the purpose of research and private study only. The thesis may not be reproduced elsewhere without the permission of the Author.

THE DEVELOPMENT OF THE BOVINE PLACENTOME AND ASSOCIATED STRUCTURES DURING GESTATION

A thesis submitted in partial fulfilment of the requirements for the degree of

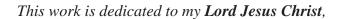
Doctor of Philosophy in Veterinary Science

Massey University, Palmerston North, New Zealand.

Folusho Doris Adeyinka

2012

Dedication



"Who is the beginning and the end"

In loving memories

My late dad, 'Samuel Oyin Oyedepo'

My late Kiwi dad 'William Bruce Teulon'

Thank you for the inspirations you have given to me.

Abstract

Placental development is a key influencer of fetal growth and development. However, limited information exists on many basic aspects of bovine placental development and the factors which affect it. To resolve this dearth of knowledge, studies of the bovine placenta were conducted to elucidate the relationship between its development and that of the fetus throughout gestation.

The first study investigated the effects by maternal nutrient restriction of two different groups of well fed heifers just prior to mating in two consecutive years to give an overall moderate weight gain during the first trimester averaging approximately 500g/day for controls compared to around 50g/day in the restricted groups Data obtainedby Day 90 of gestation, were subjected to principal component and factor analyses to evaluate the effect of nutrient restriction on placental growth. Placental growth was not directly affected by maternal nutrient restriction over the first 90 days of gestation, suggesting that significant underfeeding with weight loss is needed before placental development is affected. The study also showed that caruncle number is a major determinant of placental mass and, probably consequently, fetal mass.

The second study investigated changes in the relative contributions of fetal and maternal tissue to placentomes throughout pregnancy, using abattoir-collected material from Days 100 to 225 of gestation. Weights were measured and volumes were estimated using an air and water displacement method. Placentome number increased between Days 100 and 170 of gestation, but decreased thereafter. Mean placentome density did not show any biologically-significant variation over pregnancy. However, the contribution of maternal tissue (as determined through both weight and volume estimations) increased more rapidly with advancing gestation than did that of fetal tissue; with the consequence that maternal tissue weights were significantly greater than fetal weights by 200 days of pregnancy. The third study built upon these results by measuring placentome size *in-vivo* by trans-rectal ultrasound of dairy cows between Days 60 and 180 of pregnancy. To try to maximise the repeatability of measurements of placentome size, only those closest to the cervix were selected. The results of this study showed that there was a significant increase in placentome size between Days 60 and 180 of gestation, but that, a limits-of-agreement

analysis showed that placentome size was insufficiently closely associated with gestation age to be used as an accurate predictor of gestation age.

The final two studies examined the central zone of the feto-maternal interface of the placentome in greater detail; again using abattoir-collected material over similar period as in Study 2. In the first of these, (Study 4) stereology was used to estimate the relative volume densities, surface densities and total surface areas of the fetal and maternal components of bovine placentomes. The final study used lectin (*Dolichos buflorus* (DBA), Glycine max (SBA) and Phaseolus vulgaris leukoagglutinin (PHA-L)) histochemistry to attempt to characterize and quantify the distribution and origins of glycoproteins within the feto-maternal interface, with particular reference to the role of the binucleate cell. This was the first time that the lectin-binding properties of the bovine placetome had been objectively quantified throughout the second and third trimesters of pregnancy. Whilst the relative volume densities and surface densities of the tissues of the feto-maternal interface of the placentomes (i.e. binucleate cells, fetal trophoblast, fetal connective tissue, maternal connective tissue and maternal epithelium) did not change with gestational age, the total surface area of the feto-maternal interface increased throughout pregnancy. The presence of glycoprotein, as inferred from the patterns of lectin staining, was confined to fetal trophoblast and maternal epithelium and, in the case of DBA and, particularly, SBA, was especially prominent in binucleate cells. The latter staining probably reflects changes in the patterns of production of a key fetal regulator of maternal metabolism, placental lactogen, a glycoprotein whose origin from binucleate cells has previously been established.

Whilst it has long been established that placental size increases as pregnancy advances, this research has shown that the relationship between advancing gestational stage and placental mass is not a simple linear relationship, and even the combination of placentome size and number is not simply related to fetal size. This is, as the results of this thesis have shown, because of differential growth of the fetal and maternal components of the placentome, accompanied by progressive development of the critical interface between the mother and fetus at the central zone of apposition. It is believed that these studies have shown that in future a combination of ultrasonography, stereology and lectin histochemistry techniques could be used to quantify structural and cellular changes in the bovine placenta during gestation. This will be of value to underpin future investigations of situations in which

placental activity may be impeded to the detriment, not only of fetal growth, but also of the metabolic environment of the ensuing adult animal.

Acknowledgements

I give thanks to the Almighty God for giving me the strength, ability and wisdom to complete this work, without Him, I am nothing.

I would like to thank my chief supervisor, Dr Richard Laven, for his assistance and support from the beginning of this study right through to the end. Thank you for your brilliant ideas and for bringing out the best in me, especially my statistical skills. I am privileged to be cosupervised by Prof Tim Parkinson, I have learnt so much from you. I am very grateful for all your time, despite your busy schedule, your advice and learning from your wide scope of knowledge. Thanks to Dr Kevin Lawrence for your statistical advice and help during this study. I am honoured to have such a great team of supervisors.

I am thankful to Dr Matthew Perrot, Mike Hogan, Evelyn and Eugene for their help with histology. You are such a great team to have in the Institute. My sincere thanks to the Institute of Veterinary, Animal and Biomedical Science for regular postgraduate funding and providing me the opportunity to attend a conference in Australia. I would also like to thank the postgraduate office headed by Prof Kevin Stafford and the administrative section. Thanks to Debbie Hill, for all your assistance and willingness to help. You are one of the best administrators I have met. I can't forget Kristen Story, who is so supportive and full of smiles.

Very big thanks to Massey University for the Hardship Bursary and the Doctoral Alumni Bursary, which was of great help in paying my fees. I am also grateful to the prestigious Colin Holmes Inaugural Dairy Scholarship for the financial support and for allowing us to conduct part of the research at the Westpac research station supported by DairyNZ.

I would like to thank all my friends and office mates from IVABS, Chemistry, IFNHH, Aghort, Economics and Finance; Sharini, Lydia, Amy, Ali, Kruno, Gabriella, Maria, Sharifah, Sara, Asmad, Linda Laven, Lisanne, Santosh, Soffalina, Farihan, Mazidah, Noveline, Uttara, Beatrice, Jenny, Steve, Penny, Geraldine, Graham, Kate, Hope, Sue, Ganga, Edith, Yeshpwal, Deepa and many others. Thank you for always being there for me and for your help in putting the thesis together. Special thanks to my line manager, Mr

Andy Trow, for being so understanding and putting up with me for the last three years in Chemistry department.

My sincere thanks to my church members and friends from Emmanual Congregational church who stood by me, prayed and helped tremendously for the last few years. I will always remember my late Kiwi dad, who would have loved to see me finish this work. Thanks to my Kiwi mums and their families, Rosemary, Reine, and Nola. I would also like to thank my son's soccer team, Ruahine football club and especially Grant and Debra for taking care of KK while I was busy or out of town. Thanks to Bill Rowe for dropping and picking my kids up from school.

I am grateful to my family back in Nigeria, my mum, sisters, brother, uncle, cousins, nephews nieces and and my wonderful brother in-laws (Dapo Adeleke, Raphel Folorunsho and David Paul) for their constant calls, concern and prayers, I appreciate you all. Thanks to my friends, Dupe Orunmuyi, Taiye Olugbemi, Chris Daudu, Lekan Banwo, Joshua Ogunwole, Garce Jokthan and many others. My thanks go to Ahmadu Bello University for the study leave and fellowship granted to me. I also remember my 'Niaja kiwi' friends and family, the Adesanya's, Adelowo's, Folorunsho's, Ejiwale's, Awoshola's, Aruwa's, Beckleys and many others. My special thanks to my children, Samuel, Grace, Debra and KK for bearing with me through these years and taking care of themselves. You are the best kids anyone could ever ask for, thank God for you all. Lastly, but more important, I extend my thanks to my husband, Isaac for the support, statistical help and encouragement during the entire period of my study, I appreciate you.

Table of contents

Abstract	i
Acknowledgements	iv
Table of contents	vi
List of Figures	X
List of Tables	X
Chapter One Introduction	1
Chapter Two Literature review	5
2.1. Formation of the bovine placenta	5
2.1.1. Gross morphology of the bovine placenta	6
2.1.2. Placentome structure	6
2.2. Morphometry of the bovine placenta	14
2.2.1. Estimation of placentome growth in vivo	14
2.3. Histology of the bovine placenta	23
2.3.1. Placentome development	23
2.3.2. Trophoblast cells of the feto-maternal interface	24
2.3.3. Quantifying binucleate cell number and surface area of the placenta du gestation	_
2.3.4. Glycoprotein production during pregnancy	30
2.3.5. Lectin	31
2.3.6. Lectins and the Ruminant placentome	32
2.4. Overall conclusion	36
Chapter Three Factors Influencing Placental Morphometry in the First Trimester Pregnancy in Angus Cows	
3.1. Introduction:	39
3.2. Materials and Methods	41
3.2.1. Animals and treatments	41
3.2.2. Tissue Collection	41
3.2.3. Statistical Analysis	41
2.2 Pagulta	42

3.3.1. Least square means of placental variables	42
3.3.2. Correlation	43
3.3.3. Principal Component Analysis	44
3.3.4. Factor Analysis	44
3.4. Discussion	48
Chapter Four The Effect of Gestational Age on the Density of the Bovine Placentome	50
4.1. Introduction	50
4.2. Materials and methods	52
4.2.1. Tissue collection and sampling	52
4.2.2. Recording.	52
4.2.3. Statistical analysis	53
4.3. Results	54
4.3.1. Placentome Number.	54
4.3.1. Total Placentome weight	54
4.3.2. Caruncle and cotyledon weight	61
4.3.3. Total Placentome volume	65
4.3.4. Individual placentome volume.	67
4.3.5. Caruncle and cotyledon volume	68
4.3.6. Overall mean placentome density	71
4.4. Discussion	76
4.5. Conclusion	79
Chapter Five Determination of Gestational Age in Cattle Using Trans-rectal Ultrasomessurement of Placentomes.	
5.1. Introduction	80
5.2. Material and Methods	81
5.2.1. Animals	81
5.2.2. Ultrasonography examination	81
5.2.3. Measuring placentome size	82
5.2.4. Statistical analysis	83
5.3. Results	84
5.3.1. Descriptive statistics	84

5.3.2. Correlations between placentome dimensions and days pregnant	86
5.3.3. Mixed model regression equations	87
5.3.4. Assessment of agreement	88
5.4. Discussion	94
Chapter Six The Use of Stereology Method to Estimate the Volume of Feto-Neuronge Area of the Bovine Placentome During Gestation:	
6.1. Introduction	98
6.2. Materials and Methods	99
6.2.1. Animals and tissue sampling	99
6.2.2. Tissue Preparation and Histological Techniques	99
6.2.3. Stereology	100
6.3. Results	102
6.3.1. Relative volume densities (Vv)	102
6.3.2. Binucleate cell (BNC)	105
6.3.3. Fetal Trophoblast	105
6.3.4. Fetal Connective Tissue.	106
6.3.5. Maternal Connective Tissue (MC)	107
6.3.6. Maternal Epithelium (ME)	107
6.3.7. Maternal components (Maternal connective tissue + Maternal epithelium)) 109
6.3.8. Surface density	109
6.3.9. Total volumes and surface areas of placentome and components	109
6.3.10. Comparison between stereology and water displacement in estimates volume fetal and maternal tissue within the placentome	
6.4. Discussion	116
Chapter Seven The Use of Lectins to Study the Development of the Bovine Plac During Gestation	
7.1. Introduction	120
7.2. Materials and Methods	121
7.2.1. Animals and tissue sampling	121
7.2.2. Lectin histochemistry	122
7.2.3. Processing	123
7.2.4. Statistical analysis	124

7.3. Results	125
7.3.1. Validation of image analysis of binding intensity	125
7.3.2. Patterns of lectin binding to placentome tissue	126
7.4. Discussion	138
Chapter Eight General Discussion	141
References	154

List of Figures

Figure 2.1: Diagrammatic representation of a normal bovine placentome (Adapted from
Mossman, 1987) (ARC: arcade chorioallantois, ENDOMET: endometrium, CH ALL:
chorioallantois
Figure 2.2: Schematic illustration of placentome shapes seen in bovid ruminants showing
the maternal caruncular tissue as black and the fetal cotyledonary tissue as white. (A) Flat
placentome with caruncular tissue attached to flat endometrium. (B) Normal convex
bovine placentome with caruncular tissue attached to endometrial stalk. (C) Concave
placentome- typical of ovine ruminants (Adapted and modified from Liu et al. (2010) 9
Figure 2.3: Change in (A) caruncular and cotyledonary weights and (B) fetal and
placentomal weights by day of gestation in cows. In A, the blue line represents total
caruncular weight and the red line total cotyledonary weight. In B, the solid line represents
the fetal weight and the broken line total placentome weight. (Adapted from Reynolds et
al., 1990)
Figure 3.1: A two dimensional Principal Components graph showing the distribution of the
principal component scores for treatment groups (Low and moderate) within the 1st and
2nd principal components
Figure 4.1: Change in total number of placentomes from Days 100 to 225 of gestation.
Data from 24 uteri. The red line indicates the line of best fit
Figure 4.2: Relationship between the total weight of placentomes and gestational age. The
black line shows the best line of fit; equation in Table 4.2. 58
Figure 4.3: Relationship between ratio of predicted to actual placentome number and ratio
predicted to actual mean placentome weight. The black line shows the best line of fit;
predicted values were calculated using the equations in Table 4.2
Figure 4.4: Box plots of weight (grammes) of ten randomly selected placentomes against
gestational age (as estimated using fetal crown-rump length). Data from 24 uteri; two uteri
were collected with estimated gestational ages of 122, 134, 151, 198 and 200 days. The
black line (horizontal) in the box plot represents the mean for each uterus; the black vertical
line above and below each box plot represents the range or spread of the data; the blue box
represent the interquartile range or width of the data

Figure 4.5: Comparison of mean placentome weight (as calculated from all placentomes;
blue markers) and mean weight of ten selected (provided it was >15mm in size) individual
placentomes. 61
Figure 4.6: Box plots of weight (g) of caruncles dissected from ten randomly selected
placentomes against gestational age (as estimated using fetal crown-rump length). Data
from 24 uteri; two uteri were collected with estimated gestational ages of 122, 134, 151,
198 and 200 days. The black line (horizontal) in the box plot represents the mean for each
uterus; the black vertical line above and below each box plot represents the range or spread
of the data; the blue box represent the interquartile range or width of the data
Figure 4.7: Box plots of weight of cotyledons dissected from ten randomly selected
placentomes against gestational age (as estimated using fetal crown-rump length). Data
from 24 uteri; two uteri were collected with estimated gestational ages of 122, 134, 151,
198 and 200 days. The black line (horizontal) in the box plot represents the mean for each
uterus; the black vertical line above and below each box plot represents the range or spread
of the data; the blue box represent the interquartile range or width of the data
Figure 4.8: Relationship between individual cotyledon weight and caruncle weight
between Days 100 to 225 of gestation. The black line indicates a line of best fit for the
relationship between the fetal and maternal tissue while the red line is the line of identity,
i.e. if cotyledon weight were equal to caruncle weight.
Figure 4.9: Relationship between the total volume of placentomes and gestational age.
Data from 24 uteri. The black line shows the best line of fit; equation in Table 4.2 66
Figure 4.10: Relationship between total placentome weight and volume. The black dotted
line is the line of best fit and the red solid line is the line of identity
Figure 4.11: Box plots of volume(mLs) of ten randomly selected placentomes against
gestational age (as estimated using fetal crown-rump length). Data from 24 uteri; two uteri
were collected with estimated gestational ages of 122, 134, 151 198 and 200 days. The
black line (horizontal) in the box plot represents the mean for each uterus; the black
vertical line above and below each box plot represents the range or spread of the data; the
blue box represent the interquartile range or width of the data
Figure 4.12: Comparison of mean placentome volume (as calculated from all placentomes;
blue markers and solid line as line of best fit) and mean weight of ten selected (provided

it was >15 mm in size, red markers and solid line as line of best fit) individual placentomes.
Figure 4.13: Box plots of volume (mLs) of caruncle dissected from ten randomly selected
placentomes against gestational age (as estimated using fetal crown-rump length). Data
from 24 uteri; two uteri were collected with estimated gestational ages of 122, 134, 151,
198 and 200 days. The black line (horizontal) in the box plot represents the mean for each
uterus; the black vertical line above and below each box plot represents the range or spread
of the data; the blue box represent the interquartile range or width of the data
Figure 4.14: Box plots of volume (mLs) of cotyledon dissected from ten randomly selected
placentomes against gestational age (as estimated using fetal crown-rump length). Data
from 24 uteri; two uteri were collected with estimated gestational ages of 122, 134, 151,
198 and 200 days. The black line (horizontal) in the box plot represents the mean for each
uteri; the black vertical line above and below each box plot represents the range or spread
of the data; the blue box represent the interquartile range or width of the data
Figure 4.15: Relationship between individual cotyledon volume and caruncle volume from
Days 100 to 225 of gestation. The black line indicates a line of best fit for the relationship
between the fetal and maternal tissue while the red line is the line of identity, i.e. if
cotyledon volume were equal to the caruncle volume
Figure 4.16: Relationship between the mean density of all placentomes (total placentome
weight/total placentome volume) and gestational age. Data from 24 uteri. The black line
shows the line of best fit; equation in Table 4.2. Differentiating the equation indicates that
the minimum placentome density was attained on Day 162 of gestation when the density
was 0.95 g/mL
Figure 4.17: Box plots of density (g/mLs) of ten randomly selected placentomes against
gestational age (as estimated using fetal crown-rump length). Data from 24 uteri; two uteri
were collected with estimated gestational ages of 122, 134, 151, 198 and 200 days. The
black line (horizontal) in the box plot represents the mean for each uterus; the black vertical
line above and below each box plot represents the range or spread of the data; the blue box
represent the interquartile range or width of the data
Figure 4.18: Box plots of density (g/mLs) of caruncles dissected from ten randomly
selected placentomes against gestational age (as estimated using fetal crown-rumn length)

Data from 24 uteri; two uteri were collected with estimated gestational ages of 122, 134,
151, 198 and 200 days. The black line (horizontal) in the box plot represents the mean for
each uterus; the black vertical line above and below each box plot represents the range or
spread of the data; the blue box represent the interquartile range or width of the data 74
Figure 4.19: Box plots of density (mLs) of cotyledons dissected from ten randomly
selected placentomes against gestational age (as estimated using fetal crown-rump length).
Data from 24 uteri; two uteri were collected with estimated gestational ages of 122, 134,
151, 198 and 200 days. The black line (horizontal) in the box plot represents the mean for
each uterus; the black vertical line above and below each box plot represents the range or
spread of the data; the blue box represent the interquartile range or width of the data 75
Figure 4.20: Relationship between individual cotyledon and caruncle density. The black
line indicates the line of best fit
Figure 5.1: Images of placentomes showing measurements by using Image J software 82
Figure 5.2: Placentome length (mm) with gestation age (days) for pregnant (red line) and
non-pregnant horns in dairy cattle
Figure 5.3: Placentome area (mm²) with gestation age (days) for pregnant (red line) and
non-pregnant horns in dairy cattle
Figure 5.4: Relationship between actual gestational age and predicted gestational age
(based on log placentome length from the pregnant horn only) for cows on farm A (\blacksquare) and
Farm B (♠). Solid black line is line of identity (actual = predicted). Predicted days
pregnant = (mean log placentome length - 1.5322342) / 0.0118067
Figure 5.5: Scatterplot of difference between predicted (using log placentome length from
the pregnant horn only) and actual gestational age and the mean of the two measures. Black
line, line of best fit; red line, unadjusted limits of agreement; orange line, adjusted limits of
agreement
Figure 5.6: Scatterplot of difference between predicted (using log placentome length from
both the pregnant and non-pregnant horns) and actual gestational age and the mean of the
two measures. Black line, line of best fit; red line, unadjusted limits of agreement; orange
line, adjusted limits of agreement
Figure 5.7: Relationship between actual gestational age and predicted gestational age
(based on mean placentome length) for cows on farm A (■) and Farm B (◆). Solid line is

line of identity (actual = predicted). Predicted days pregnant = (mean placentome length +
6.11) / 0.228
Figure 5.8: Scatterplot of difference between predicted (using placentome length) and
actual gestational age and the mean of the two measures. Black line, line of best fit; red
line, unadjusted limits of agreement; orange line, adjusted limits of agreement
Figure 6.1: Illustrates a series of parallel cutting planes of 4mm thick slices of a
placentome. 100
Figure 6.2: Bovine placentome at Gestation stage 2 (126 – 150 days) showing binucleate
cells (BNC); fetal connective tissue (FC); fetal trophoblast (FT); maternal connective tissue
(MC) and maternal epithelium (ME). Masson's Trichrome
Figure 6.3: Bovine placentome at Gestation stage 2 (126-150 days) with a 9x9 point grid
generated by image analysis (Image J software) overlaid on the image. Examples of points
falling on a tissue of interest are represented by arrows (FT) fetal trophoblast; (MCT)
Maternal connective tissue. Masson's Trichrome
Figure 6.4: Bovine placentome at Gestation stage 2 (126-150 days) with cycloid grid
generated from image analysis (Image J software) overlaid on the image. Examples of
points of intersection (I) crossing the feto-maternal interface are represented by arrows.
Masson Trichrome. 104
Figure 6.5: Change in relative volume density of binucleate cells of bovine placentomes
sections from 100 to 260 days of gestation. Data from 25 uteri with a section randomly
selected from each cow and 3 fields viewed per section
Figure 6.6: Change in relative volume density of fetal trophoblast cells of bovine
placentomes sections from 100 to 260 days of gestation. Data from 25 uteri with a section
randomly selected from each cow and 3 fields viewed per section
Figure 6.7: Change in relative volume density of fetal connective tissue of bovine
placentomes sections from 100 to 260 days of gestation. Data from 25 uteri with a section
randomly selected from each cow and 3 fields viewed per section
Figure 6.8: Change in relative volume density of maternal connective tissue of bovine
placentomes sections from 100 to 260 days of gestation. Data from 25 uteri with a section
randomly selected from each cow and 3 fields viewed per section

Figure 6.9: Change in relative volume density of maternal epithelium of placentomes
sections from 100 to 260 days of gestation. Data from 25 uteri with a section randomly
selected from each cow and 3 fields viewed per section
Figure 6.10: Change in relative volume density of maternal components of placentomes
sections from 100 to 260 days of gestation. Data from 25 uteri with a section randomly
selected from each cow and 3 fields viewed per section
Figure 6.11: Change in surface density within the feto-maternal interface per unit of
placentomes sections from 100 to 260 days of gestation. Data from 25 uteri with a section
randomly selected from each cow and 3 fields viewed per section
Figure 6.12: Change in total volume of placentome components; binucleate cells (♠), fetal
trophoblast (■), fetal connective tissue (▲), maternal connective tissue (•) and maternal
epithelium (•) from 100 to 260 days of gestation
Figure 6.13: Change in estimated total surface area of the feto-maternal interface (FMI) of
the bovine placentome from 100 to > 200 days of gestation. Data from 25 uteri with a
section randomly selected from each cow and 3 fields viewed per section
Figure 6.14: Change in the volume of fetal and maternal tissue in the placentome during
gestation as estimated using stereology (fetal [■]; maternal [■]) and water displacement
(fetal $[\spadesuit]$; maternal $[\spadesuit]$).
Figure 6.15: Effect of gestational age on ratio of fetal to maternal tissue (by volume) in
placentome estimated using water displacement (�) or stereology (�). Solid line is line of
best fit for water displacement ($R^2 = 0.333$), there was no significant association for
stereology (R^2 =0.01). 115
Figure 7.1: Lectin (DBA) staining of the feto-maternal unit showing the fetal and
maternal components; binucleate cell (BNC), maternal epithelium (ME), uninucleate cell
(UNC), fetal villi (FV). Magnification 400x. 124
Figure 7.2: Unprocessed (a) and processed images (b) of DBA lectin binding to placental
tissue visualised at magnification 400x. In Figure 7.2a, lectin binding is seen as area of
yellow, orange and gold fluorescence. In Figure 7.2b, areas coloured black indicate
minimal binding, green areas indicate medium binding, and red areas indicate maximum
binding 124

Figure 7.3: Mean fluorescence intensity per pixel for all lectin stains throughout all	
gestational stages, separated by image analysis into bright (intense binding; top group),	
medium (less intense binding; middle group) and dark (minimal binding) intensities. Red	
line, SBA binding; green line, PHA-L; blue line, DBA	5
Figure 7.4: Mean (± SEM) fluorescence intensity for the binding of PHA-L to bovine	
placentomes between Days 100 and 260 of gestation	6
Figure 7.5: Binding of fluorescent-labelled biotinylated PHA-L to placentome tissue at	
Gestation Stage 1 (Days 100-125). Image captured at 400 x magnification	7
Figure 7.6: Binding of fluorescent-labelled biotinylated PHA-L to placentome tissue at	
Gestation Stage 2 (Days 126-150). Image captured at 400x magnification	7
Figure 7.7: Binding of fluorescent-labelled biotinylated PHA-L to placentome tissue at	
Gestation Stage 3 (Days 151-175). Image captured at 400x magnification	8
Figure 7.8: Binding of fluorescent-labelled biotinylated PHA-L to placentome tissue at	
Gestation Stage 4 (Days 176 -200). Image captured at 400x magnification	8
Figure 7.9: Binding of fluorescent-labelled biotinylated PHA-L to placentome tissue at	
Gestation Stage 5 (Days 201-260). Image captured at 400 x magnification	9
Figure 7.10: Mean (± SEM) fluorescence intensity for the binding of DBA to bovine	
placentomes between Days 100 and 260 of gestation. The red dotted line shows the	
quadratic line superimposed on the data graph	1
Figure 7.11: Binding of fluorescent-labelled biotinylated DBA to placentome tissue at	
Gestation Stage 1 (Days 100-125). Image captured at 400x magnification	1
Figure 7.12: Binding of fluorescent-labelled biotinylated DBA to placentome tissue at	
Gestation Stage 2 (Days 126-150). Image captured at 400x magnification	2
Figure 7.13: Binding of fluorescent-labelled biotinylated DBA to placentome tissue at	
Gestation Stage 3 (Days 151-175). Image captured at 400x magnification	2
Figure 7.14: Binding of fluorescent-labelled biotinylated DBA to placentome tissue at	
Gestation Stage 4 (Days 176-200). Image captured at 400x magnification	3
Figure 7.15: Binding of fluorescent-labelled biotinylated DBA to placentome tissue at	
Gestation Stage 5 (Days 201-260) Image captured at 400x magnification 13	3

Figure 7.16: Mean (± SEM) fluorescence intensity for the binding of SBA to bovine	
placentomes between Days 100 and 260 of gestation. The blue dotted line shows the	
quadratic line superimposed on the data graph.	135
Figure 7.17: Binding of fluorescent-labelled biotinylated SBA to placentome tissue at	
Gestation Stage 1 (Days 100-125). Image captured at 400x magnification	135
Figure 7.18: Binding of fluorescent-labelled biotinylated SBA to placentome tissue at	
Gestation Stage 2 (Days 126-150). Image captured at 400x magnification.	136
Figure 7.19: Binding of fluorescent-labelled biotinylated SBA to placentome tissue at	
Gestation Stage 3 (Days 151-175). Image captured at 400x magnification.	136
Figure 7.20: Binding of fluorescent-labelled biotinylated SBA to placentome tissue at	
Gestation Stage 4 (Days 176-200). Image captured at 400x magnification.	137
Figure 7.21: Binding of fluorescent-labelled biotinylated SBA to placentome tissue at	
Gestation Stage 5 (Days 201-260). Image captured at 400x magnification.	137

List of Tables

Table 2.1: Summary of accuracy or positive predictive value of ultrasound in early
pregnancy diagnosis in cattle
Table 2.2: Association between fetal parameter measured and accuracy of determining
gestational age
Table 2.3: Definition of symbols used in stereology 27
Table 2.4: Summary table showing types of lectins, specificity, results and references 34
Table 3.1: Means of Placental variables with Standard error (±SE) for low and moderate
diet treatment
Table 3.2: Correlation between cotyledon and caruncle weight and other variables
Table 3.3: Result of Factor Analysis: Factors and Factor Loadings* 46
Table 4.1: Comparison between gestational stages in mean (SEM) gestational age
placentome number, total placentome weight and volume and mean density 55
Table 4.2: Relationship, as modelled using GLM, between gestational age (days) and
weight (g), volume (mL) or density (g/mL) of placentomes and placentome components
Data from 24 uteri, and based on either all placentomes in the uterus (total) or ten randomly
selected individual placentomes. 57
Table 4.3: Correlation (p-value) between total number of placentomes per uterus with total
placentome weight, volume and overall mean density of placentomes
Table 4.4: Correlation of placentome and placentome component weight, volume and
density. Data from 10 individual placentomes randomly selected (excluding placentomes
<15mm in size) from the uteri of 24 cattle. All correlations were significant (P<0.001) 63
Table 5.1: Mean ± Standard deviation placentome length and area per breed on the
pregnant and the non-pregnant uterine horns.
Table 5.2: Mean \pm Standard deviation placentome length and area per breed for the
pregnant and the non-pregnant horn.
Table 5.3: Estimates of fixed effects of Days pregnant, breed, age, farm and horn (or
length of placentome) 87
Table 6.1: Volume densities (%) of placentome components and surface density of feto-
maternal-interface (FMI) of bovine placentomes in each stage of gestation

Table 6.2: Total volume densities (mL) and Total surface area of feto-maternal interface
(FMI) (means \pm SE) of bovine placentomes in each stage of gestation
Table 6.3: Effect of stage of gestation on mean volume of fetal and maternal placentome
tissue estimated using either stereology or water displacement (Chapter 4 of the present
study)114